
PHYSICS OF ELEMENTARY PARTICLES
AND ATOMIC NUCLEI. EXPERIMENT

Technological Process of Assembly and QA Testing of Silicone Tracking Modules with Silicon Strip Sensor

A. D. Sheremetev^{a, *}, V. V. Leontiev^a, D. V. Dementev^a, M. O. Shitenkov^a, and Yu. A. Murin^a

^a *Veksler and Baldin Laboratory of High Energy Physics, Joint Institute for Nuclear Research,
Dubna, Moscow oblast, 141980 Russia*

**e-mail: sheremetiev@jinr.ru*

Received August 29, 2023; revised November 28, 2023; accepted November 28, 2023

Abstract—The key technological stages of assembly of silicone tracking modules with silicon strip sensors for use in the wide-aperture silicon tracking system of the BM@N experiment are considered. Methods for finding the optimal parameters for the ultrasonic linear automatic welding of aluminum microcables with a silicon sensor are described. The methodology and results of intermediate QA testing during the assembly of the silicone tracking module are presented. The method of mounting unpackaged microcircuits on a board is described. The results of the preproduction assembly of silicone tracking modules are presented.

DOI: 10.1134/S1547477124700456

INTRODUCTION

Tracking systems based on silicon coordinate-sensitive sensors are widely used in high-energy physics experiments to reconstruct the trajectories of secondary particles, their moments, and vertices of birth, making it possible to achieve record spatial resolution and have the necessary speed for installing them at minimal distances from the particle source. The high granularity of silicon tracking systems results in a large number of readout electronics channels, which can reach several billion in modern experiments. The design of such tracking systems involves the use of lightweight support trusses made of carbon composite materials, on which sensors are mounted in the form of tiles.

Typically, the minimum detecting element of a system is a module consisting of one or more sensors and readout electronics. When strip sensors are used in modern physics facilities, it is necessary to move the readout electronics away from the sensitive area of the sensor in order to minimize the amount of material in the path of secondary particles and reduce the radiation load of the electronics. The DØ experiment (Fermilab, United States), forced to upgrade its sensor, was the first to encounter this technically nontrivial problem [1]. Solving this problem is complicated by the need to transmit an ultralow amplitude charge signal (~ 3.6 fC for sensors with a thickness of $300\ \mu\text{m}$) from the sensor to the input paths of readout microcircuits with minimal losses, without introducing additional substances that degrade the spatial resolution of the system. In addition, sensors with stripe pitches of less than $100\ \mu\text{m}$ are used in modern facilities. This

requires the development and production of specialized microcables of considerable length (up to 50 cm) adapted to the topology of the sensors and microcircuits used in the experiment.

In the DØ experiment, expensive long copper cables from Dyconex AG (Switzerland) [1] were used in the construction of the L0 layer of the central tracking system [2]. At the same time, the main modules of the central tracker with strip sensors were already connected to the readout electronics using short aluminum microcables on a polyimide base manufactured by LTU (Kharkiv, Ukraine). Later, CERN scientists successfully used short aluminum LTU microcables to create modules of two outer layers in the first version of the ITS inner tracking system of the ALICE experiment at CERN [3].

Considering the experience of the ALICE and DØ experiments, it can be concluded that the abandonment of the use of copper cables in favor of cheaper and lighter ones was completely justified by the time work began on creating large-area silicon tracking systems. Calculations of noise characteristics associated with an increase in cable track resistance when moving from copper to aluminum were small [1]. The use of aluminum conductors allows the use of ultrasonic tape automated bonding (TAB) [4] to connect a microcable to contact pads on silicon crystals. It is also important that the radiation length (X_0) for aluminum is more than twice as high as for copper, which reduces the secondary scattering of particles and radiation losses in the tracking system.

Special requirements are placed on inner vertex tracking systems in modern experiments aimed at

studying the properties of superdense baryonic matter in collisions of heavy ions. An example is the silicon tracking system being created at the CBM experiment (FAIR, Germany) [5]. This system must measure tracks of secondary particles under conditions of high speed (interaction frequency is up to 10 MHz) and high multiplicity of secondary particles (up to 700 in Au + Au collisions at energies of 10 GeV per nucleon), must be able to operate under conditions of high radiation loads (up to 10^{14} MeV neutron equivalents per square centimeter), and provide a spatial resolution for secondary particle tracks of no worse than 25 μm . The design of the CBM silicon tracking system includes eight planes consisting of modules based on silicon strip sensors mounted inside a dipole magnet. Each module consists of a sensor, two boards with readout electronics, and a set of ultralight (0.23% X_0) polyimide-based aluminum microcables. The design of the tracking module and the method of serial assembly of such modules were developed as part of the collaboration between the CBM and the silicon tracking system development group of the BM@N experiment, where it was also planned to use tracking modules of a similar design.

This article describes a technique for assembling tracking modules consisting of silicon strip sensors and readout electronics connected to the sensor channels using ultralight aluminum microcables. The results of QA testing modules during and after assembly and the results obtained after assembling experimental tracking modules for the future silicon tracking system of the BM@N experiment are given.

MAIN COMPONENTS OF THE BM@N TRACKING MODULE

The silicon tracking system of the BM@N experiment is part of a hybrid tracker located inside the SP-41 dipole magnet. Currently, the hybrid tracker consists of four planes based on double-sided silicon sensors (FW-Si) and seven planes of GEM (gas electron multipliers) sensors, in front of which it is planned to install four silicon tracking systems (STSs) with a larger aperture [6]. The STS should consist of 292 track modules. A photograph of the module with the main components is shown in Fig. 1.

The key component of the tracking module is a strip sensor, which was designed for the tasks of the CBM experiment [7]. When assembling tracking modules, Hamamatsu Photonics K.K sensors [8] with sizes of $62 \times 62 \text{ mm}^2$ and $42 \times 62 \text{ mm}^2$ are used. The sensor thickness is $320 \pm 15 \mu\text{m}$. The sensors are manufactured using planar technology on wafers of high-resistivity n -type silicon grown by float zone melting (FZM) with a resistivity of $\sim 8 \text{ k}\Omega \text{ cm}$. Each side of the sensor contains 1024 microstrips spaced at 58 μm pitches. On the n side, the strips are located parallel to the edges of the sensor ($\theta_n = 0^\circ$); on the p side, the

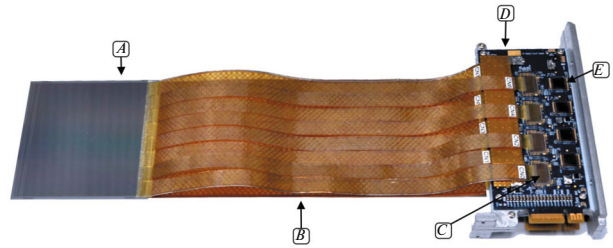


Fig. 1. General view of the BM@N STS silicon tracking module. (A) Silicon double-sided microstrip sensor, (B) ultralight aluminum polyimide microcables, (C) STS-XYTER application-specific integrated circuit (ASIC), (D) microcircuits of LDO regulator, and (E) FEB interface board.

strips are located at an angle of $\theta_p = 7.5^\circ$. Short strips located in opposite corners of the sensor are connected using a second layer of metallization on the surface of the sensor (Fig. 2).

The sensors have a resistance (500 k Ω) and a separating capacitance integrated into each microstrip, providing communication through the dielectric layer via alternating current between the depleted region of the strip and the metallization of the microstrip for signal reading.

A set of flat aluminum microcables is used to connect the readout electronics to the sensor strips. Such a microcable is manufactured by photolithography on FDI-A20 polyimide [9]. The amount of substance in one layer of aluminum polyimide microcables is 0.23% X_0 [10]. The thickness of the microcable is 24 μm (the thickness of aluminum is 10 μm and the thickness of polyimide is 14 μm). A 75- μm -thick polyimide mesh with 30% filling is glued over each microcable during the module assembly process, which allows for the minimum dielectric constant for a given design and thereby reduces AC coupling between adjacent conductors in the assembly. Each microcable has 64 signal conductors with a width of 40 μm and a pitch of 116 μm . The signal line resistance is 9–14 $\Omega \text{ cm}^{-1}$ and a capacity is 0.36–0.45 pF cm^{-1} [9, 10]. The topology of the ultralight microcable involves the use of TAB technology to connect conductors to contact pads on the sensor and readout electronics without the use of additional transition connections.

Signals from the microstrip sensor are transmitted to the fast readout electronics of the sensor based on the STS-XYTER ASIC [11, 12]. The chip is manufactured according to the CMOS process of UMC (United Microelectronics Corporation), 180 nm; its area is $10 \times 6.75 \text{ mm}^2$ [12]. The size of the contact pads for TAB is $180 \times 60 \mu\text{m}$ and the pitch is 116 μm . Such a high contact density is due to the use of unpackaged microcircuits. The key feature of the chip is the architecture of stream signal processing without the use of an external trigger [13]. The chip has 128 input channels of low-noise ($<1000 \text{ e/r.m.s.}$) charge-sensitive

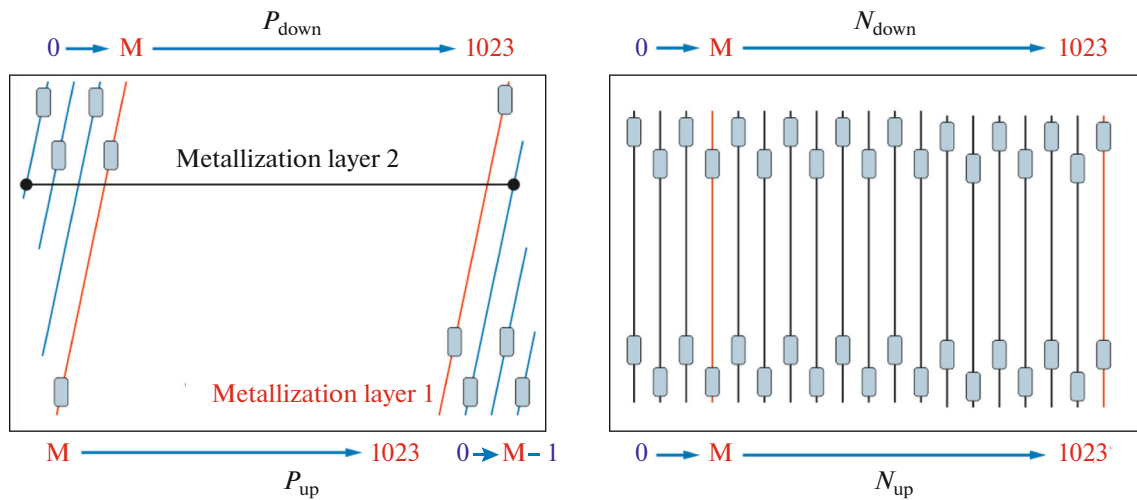


Fig. 2. Diagram of the orientation of microstrips on the sensor. On the p side of the sensor, the microstrips are connected using a second metallization layer (for a sensor with sizes of $62 \times 62 \text{ mm}^2$, the number of short strips is $M = 134$; for a sensor with sizes of $62 \times 42 \text{ mm}^2$, the number of short strips is $M = 88$).

amplifiers (CSAs), which allow reading signals with a low amplitude of 3.6 fC. After CSA, the signal is divided into two branches. One of them is used to measure the signal amplitude and determine the center of gravity of the cluster using a five-bit ADC with the ability to adjust the dynamic range of input signals from 12 to 120 fC. Another branch with faster signal generation time is intended for fixing the time stamp. The maximum throughput of the chip is 50 million events per second for 128 recording channels. STS-XYTER can handle signals of both polarities. For this purpose, an additional signal inverter is used at the output of the CSA when working with charges of negative polarity.

Two FEB interface boards (each of them contains eight STS-XYTER packaged chips) are used to read and process signals from all sensor strips. To power the readout electronics of the sensor, four specialized microcircuits of low-dropout (LDO) linear regulator in a packageless design are mounted on each FEB board during the module assembly process [14].

The tracking module design includes a silicon microstrip sensor, a set of 32 aluminum polyimide cables, 16 STS-XYTER chips, two FEB interface boards, eight packageless LDO linear regulators, six shields for readout electronics and analog microcables, and an aluminum radiator.

TECHNOLOGICAL STAGES OF ASSEMBLY OF TRACKING MODULE

The assembly of tracking modules is the most complex and lengthy technological stage of the production of a tracking system, which required the development and production of specialized high-precision tooling, the optimization of all technological stages of assem-

bly and their sequence, the integration of quality control procedures at all stages, and a construction management information system (CMIS) [15] (which makes it possible to effectively control the serial assembly of modules in geographically distant assembly centers (GSI–JINR)).

All components used in the assembly process undergo a preliminary stage of visual and functional testing, which allows one to minimize the number of defects in the production process. The technological process for assembling tracking modules includes four key assembly stages and three stages of level testing.

(1) The assembly of two FEB interface boards with LDO linear regulator's microcircuits (Fig. 3a).

(2) The assembly of sixteen microcircuits with microcables. Ultrasonic welding of STS-XYTER ASIC with two microcables for even and odd channels and testing of electrical connection. In the technological process, this assembly is designated as microcircuit–microcable (Fig. 3b).

(3) The assembly of microcircuit–microcable–sensor. Welding of sixteen microcircuits with microcables to pads on both sides of the sensor (Fig. 3c).

(4) Installation and welding of ASIC on FEB interface boards (Fig. 3d).

Installation of LDO Linear Regulator's Microcircuits on FEB Interface Boards

The LDO microcircuit is installed on the FEB circuit board using thermally conductive adhesive¹ (Fig. 4a). The adhesive is applied using a manual dis-

¹ Epoxy Technology Epo-Tek® H20E Electrically Conductive, Silver Epoxy.

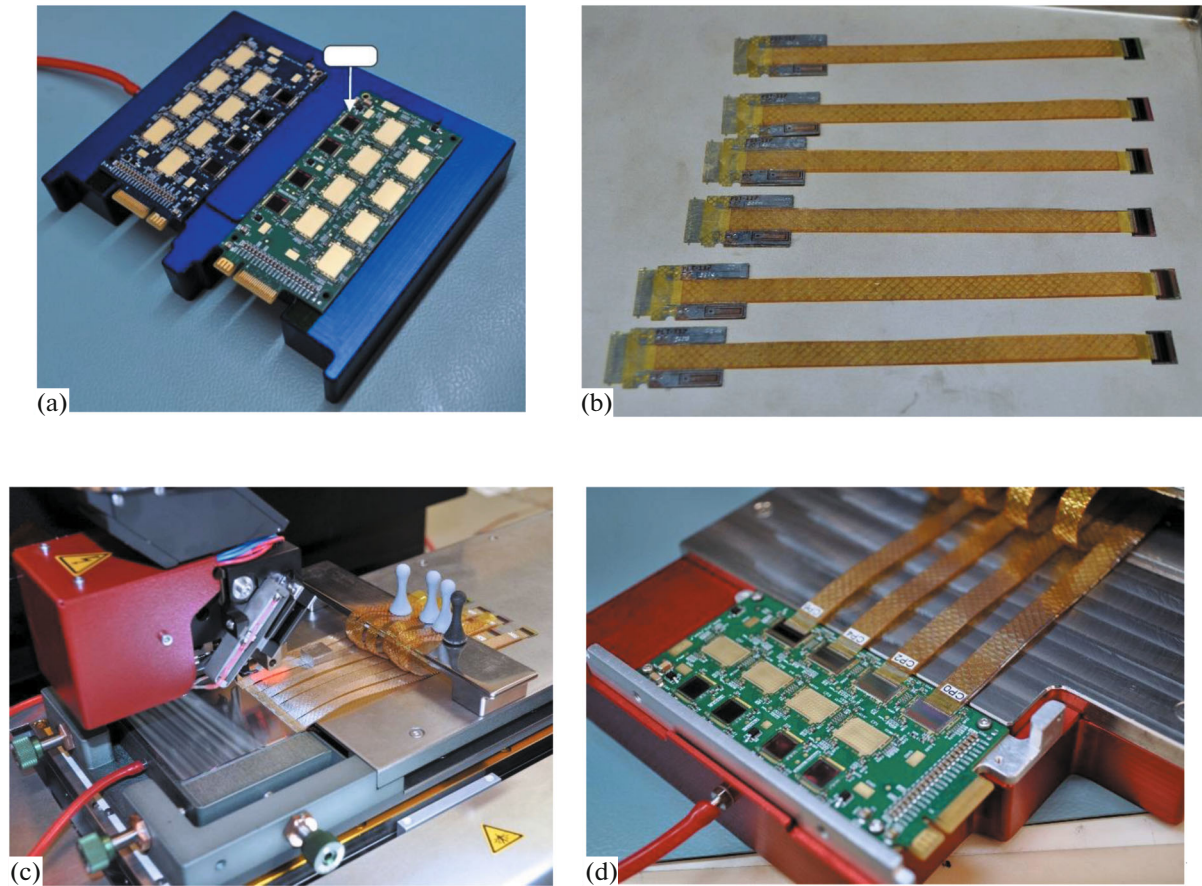


Fig. 3. Main stages of assembly of the tracking module. (a) A set of FEB boards mounted on test equipment, (b) a set of microcables assembled with STS-XYTER ASIC with a connector for testing, (c) ultrasonic microcircuit–microcable welding with a sensor, and (d) installation of the microcircuit–microcable–sensor assembly on the reading electronics board.

penser. At this stage, it is important to ensure a uniform pattern of applying adhesive to all places where the microcircuit is installed and its uniform distribution over the entire area of the microcircuit to ensure high-quality heat removal from the crystal. The method of dot application of adhesive with a dot diameter of 400 μm in increments of 800 μm was chosen experimentally. After the adhesive cures in an oven at 120°C, the contact pads on the chip and interface board are ultrasonically welded using aluminum wire with a diameter of 25 μm (Fig. 4b). At the next stage, the quality of ultrasonic connections is checked using a microconnection tensile test bench². The testing method used is destructive and involves tearing off three test welds on the assembly. During this test, the wire pullout force is measured and compared with the calculated value. For the type of wire that is used, the intrinsic value of the maximum tensile strength is 14–16 g. After testing the quality of the weld joints, the chip and weld joints are encapsulated to protect against mechanical damage and electrically insulate the conductors. Encapsulation is carried out in two

² Nordson Test & Inspection 4000 Plus Bondtester.

stages using the dam-and-fill technology [16] with adhesives³ to create a dam and as filler.⁴

After LDO encapsulation, the chips with the test load are turned on. This test is necessary to monitor the performance of LDO chips and the set maximum output current, at which protective shutdown takes place. To test LDO, an automated bench is used, which includes a power supply,⁵ electronic load,⁶ multimeter,⁷ and software written in LabVIEW [14]. An example of the test results of two LDOs after installation on a printed circuit board is shown in Fig. 5.

Ultrasonic Welding of Microcircuits for Assembly and Processing of Signals from a Sensor with Aluminum Microcables

It should be emphasized that one feature of the tracking module is the use of ultralight aluminum

³ Dymax Multi-Cure[®] 9001-E-V3.1 Resilient Encapsulant.

⁴ Dymax Multi-Cure[®] 9008 UV-Curable Flex Circuit Adhesive.

⁵ Power supply Rohde Schwarz HMP2030.

⁶ Programmable DC Electronic Load Keithley 2380.

⁷ Multimeter Keithley 2000.

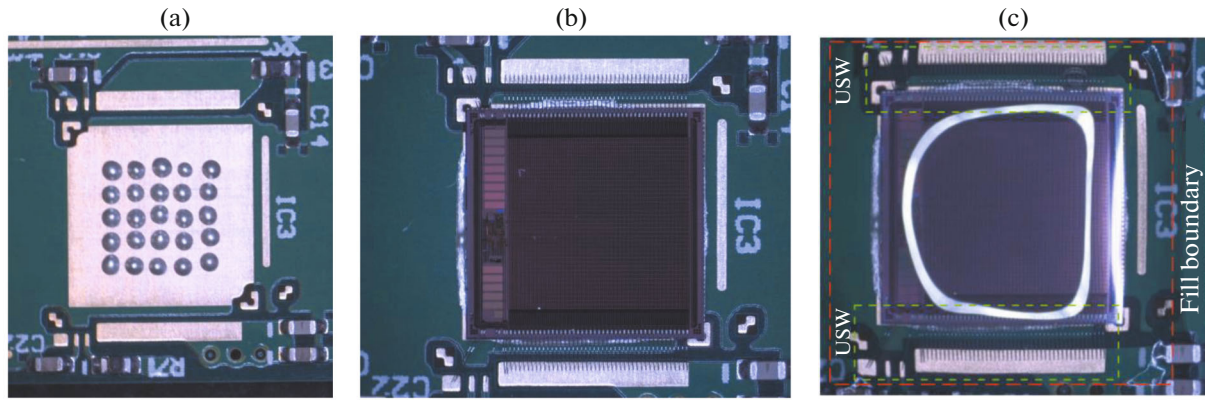


Fig. 4. Stages of assembling an LDO regulator microcircuit and an electronics board. (a) Application of thermally conducting adhesive to the FEB interface board, (b) LDO regulator microcircuit after ultrasonic welding with aluminum wire (25 μm), and (c) encapsulated microcircuit with ultrasonic welding areas and the microcircuit encapsulation boundary.

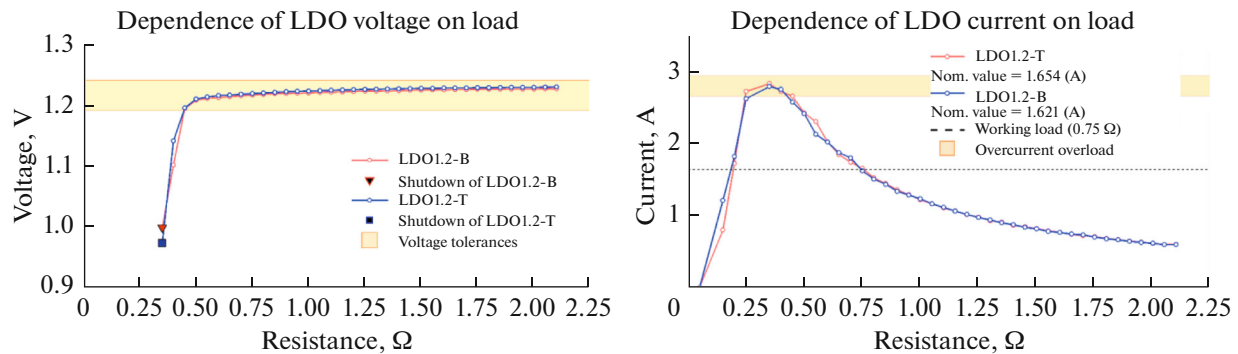


Fig. 5. Testing of two LDO microcircuits after assembly on an electronics board. Dependence of the output voltage of the microcircuit on the load resistance is shown on the left. Dependence of the output current of the microcircuit on the load resistance is shown on the right. During testing, the value of the output voltage is checked at the rated load (0.75 Ω) and the operation of the protective shutdown of the microcircuit if the specified threshold for the output current of 2.8 A is exceeded (in this case, the voltage value drops to 0.9 V). If the tests fail, the board with installed LDOs is not used for module manufacturing.

polyimide microcables, which are connected to the sensor and microcircuits using TAB ultrasonic technology [4]. This method has a number of advantages over classical ultrasonic wire welding.

(1) The number of required contact connections is two times less than when using thermosonic ball welding or thermo-compression welding.

(2) The connection of internal tensile leads is more durable.

(3) Ultrasonic welding of an aluminum plane conductor and an aluminum contact pad can be carried out without preheating the sample.

(4) The possibility of multilevel assembly in one plane and the possibility of low-profile (planar) design.

(5) For welding, it is necessary to destroy the oxide layer on the contact pad. Removing aluminum oxide from a surface requires less effort than removing copper or gold oxide. This allows one to more accurately select parameters for welding and minimize the nega-

tive impact on the structure of the crystal under the welding zone.

This technology is used when assembling the STS-XYTER ASIC with two aluminum microcables. The contact pitch on the microcable is 116 μm . The pitch of the strips on the sensor is 58 μm , so the contact pads on the sensor and ASIC are arranged in a checkerboard pattern and two layers of microcables are used to weld even and odd channels. Each microcable has 64 conductors, and the ASIC has 128 input channels.

The assembly of a microcable with a microcircuit is carried out in three stages (combining an aluminum microcable with ASIC using specialized equipment, ultrasonic welding of an aluminum microcable with a microcircuit, and testing the assembly on a bench).

The quality of the assembled products depends on the correctness and accuracy of the selected ultrasonic welding parameters (force, time, and power of ultrasonic welding). Each microcable has a test zone for

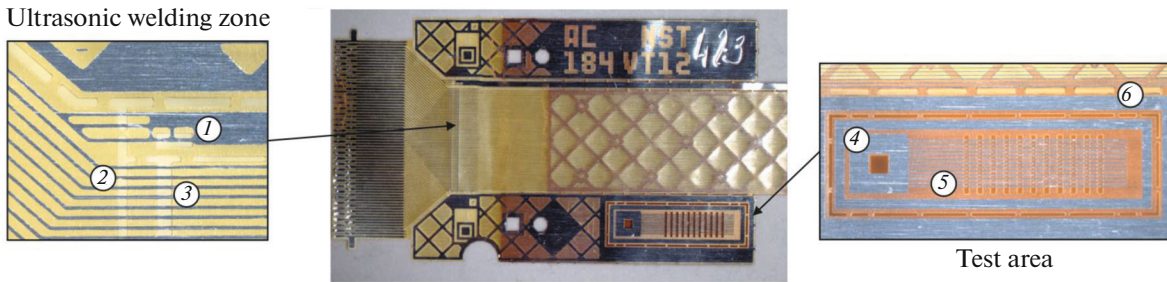


Fig. 6. Ultralight aluminum microcable with test zone. The ultrasonic welding zone includes a bias voltage supply conductor to the sensor with a USW window (1), windows for cutting off the cable test zone (2), and 64 signal aluminum conductors for USW (3). The test area includes an area for installing a tear-off tool (4), 11 windows with ten conductors for selecting USW parameters (5), and an area for cutting (6).

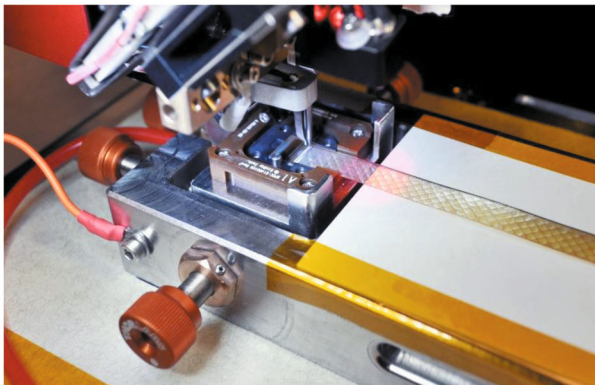


Fig. 7. Assembling of ASIC readout electronics with an ultralight aluminum microcable on an ultrasonic welding bench.

preliminary selection of parameters (Fig. 6) and a window for ultrasonic welding of contact pads on the cable.

The microcable is laid on the ASIC fixed in specialized equipment (Fig. 7) and positioned using micrometric screws. The positioning accuracy is about

5 μm . The platform for installing the microcircuit on the equipment has a positioning system for installing a test card, which allows the functional testing (measurement of idle noise) of the microcircuit on the assembly equipment.

The test area of the microcable is welded onto a silicon crystal (a microstrip sensor that has not passed functional tests) (Fig. 8a) to select ultrasonic welding parameters. Ultrasonic welding of the test zone is performed at four points, which gives more stable measurement results and reduces the likelihood of mechanical damage during installation in the test bench (Fig. 8b). After tearing off the test zone, the measured tear force is recalculated per weld point. This stage allows one to select the time, power, and force for each welded joint. The parameters are selected for a batch of microcables manufactured in one technological process. The welding quality is assessed by shear testing of the specimen in accordance with the MIL-STD-883 2011.9 standard [17]. This method is destructive, since the sample shifts and the tear force is measured during the test. Measurements are made using a Nordson Bondtester 4000 Plus (Fig. 8a).

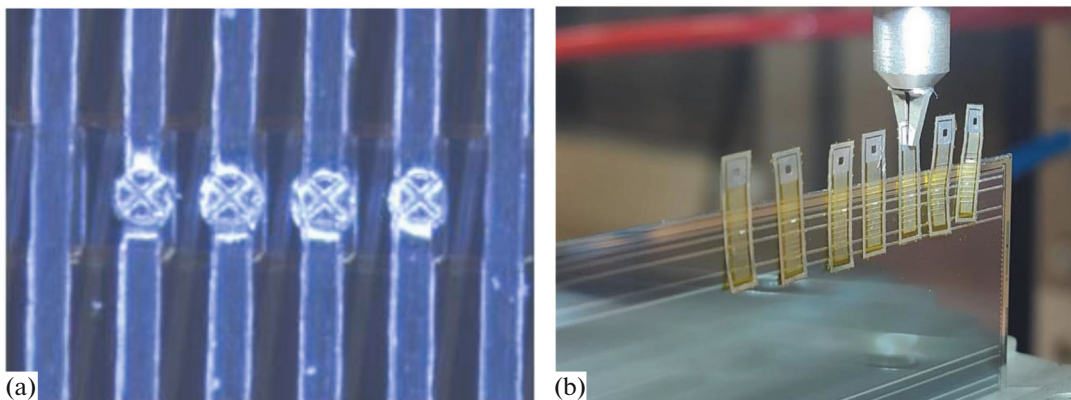


Fig. 8. (a) Silicon sensor with test samples on a tear test bench and (b) ultrasonic welding of four conductors using TAB technology.

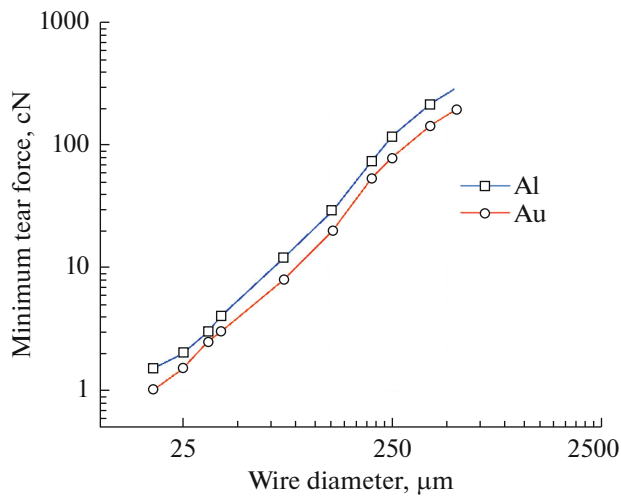


Fig. 9. Dependence of the minimum destructive tear force on the wire diameter for a gold and aluminum ultrasonic connection.

The parameters of the welded joint are set in accordance with the MIL-STD-883 2011.9 standard. The dependence of the tear force on the diameter of the aluminum wire during a welded joint is presented in Fig. 9 [17]. With a conductor cross-sectional area of $490 \mu\text{m}^2$ (corresponding to a wire diameter of $25 \mu\text{m}$), the tear force after welding should exceed 2 g . The cross-sectional area of the conductor used for welding microstrip modules is $560\text{--}595 \mu\text{m}^2$ and is determined by the etching time of the conductor during the photolithography process. Based on the cross-sectional area of the conductor in the microcable, it can be concluded that the tear force required for a quality connection must be $\geq 2.41 \text{ g}$ per conductor.

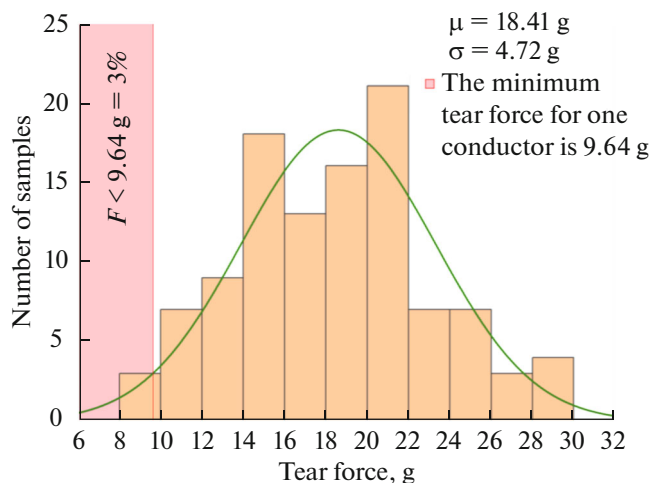


Fig. 10. Results of tear testing of aluminum microcable samples welded at four points to a microcircuit using TAB technology.

In preparation for the assembly of the STS-XYTER ASIC with flexible aluminum microcables, more than 100 tear-off test samples were tested. The mean tear force for the four-point weld test area on the chip was $18.4 \pm 0.9 \text{ g}$, which corresponds to a force of $18.4/4 = 4.6 \text{ g}$ for each conductor in the sample. The results satisfy the requirements for this stage of manufacturing and guarantee reliable mechanical and electrical connection of the microcable with the sensor and the microcircuit. The measurement results are presented in Fig. 10.

After assembling the microcircuit–microcable, functional testing is carried out using a test card [14]. In addition to checking the functionality of the microcircuit, testing makes it possible to identify idle channels, unwelded channels, or channels damaged by a static charge during assembly. The method for assessing the quality of the welded state and the performance of an individual microcircuit channel is based on measuring and monitoring the noise level in each channel of the microcircuit at each stage of module assembly. After each new assembly stage, the capacitance at the input of the CSA increases, and the noise level in a single channel increases due to this. If the noise in the channel after microcircuit–microcable assembling remains at the same level, this indicates that there is no electrical connection between the cable and the input pad of the microcircuit. If the input path was damaged during the welding process, there is no signal from this channel. The test results for one microcircuit–microcable assembly are shown as an example in Fig. 11a. The measured noise is compared with the intrinsic noise

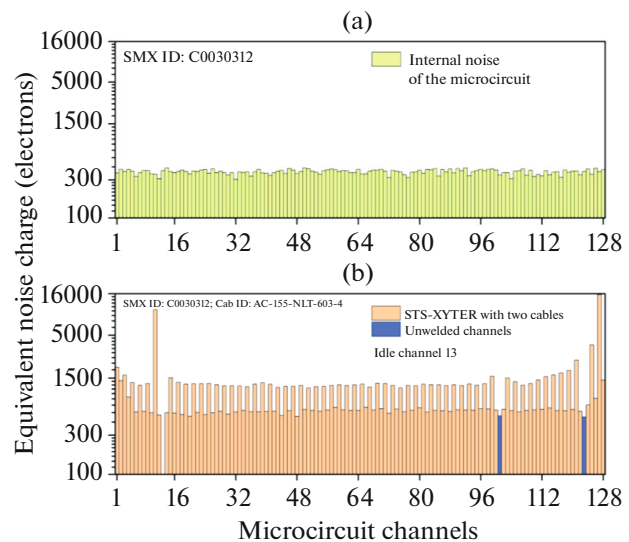


Fig. 11. Results of intermediate testing of STS-XYTER ASIC during the microcircuit–microcable assembly process. The microcircuit and microcable were tested in a test box without a shield. The difference between even and odd channels is characterized by the fact that the upper cable in the assembly is a shield for the lower cable.

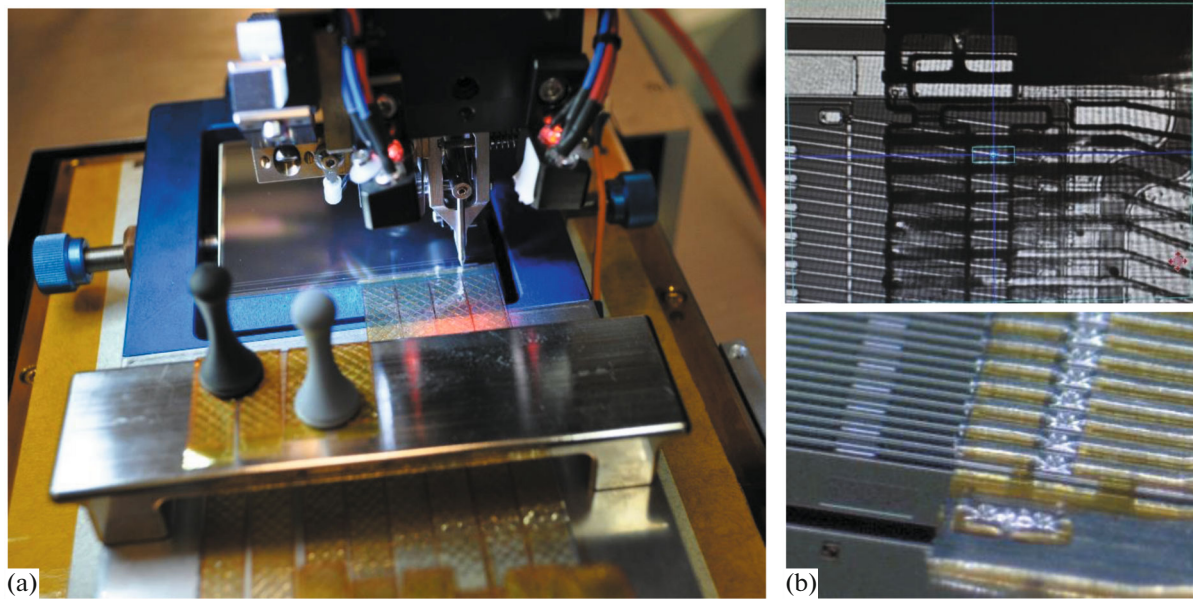


Fig. 12. (a) Ultrasonic welding of a flexible microcable with a sensor and the connection of the microcable with the sensor platform (b).

of the chip before assembly. Zero noise (channel 13, Fig. 11b) implies that there are no signals from this channel, which may be caused by static charge damage or mechanical damage during assembly. One consequence of the damage is also increased noise on the adjacent channel 11 (10248 electrons).

Intermediate testing (Fig. 11b) showed that channels 101 and 123 do not have a significant increase in noise relative to the measured intrinsic noise of the microcircuit. A slight increase in noise in the channels of the microcircuit after assembly requires additional visual checkout, since it is possible that the welding quality in these channels does not meet the assembly requirements. The electrical testing process is described in more detail in [18].

Installing Microcable Readout Electronics onto a Silicon Microstrip Sensor

The microcircuit–microcable–sensor assembly process takes place using specialized equipment. The assembly process includes four stages. They are alignment of the microcircuit–microcable assembly pads relative to the pads of the microstrip sensor, ultrasonic welding with parameters selected using samples, functional testing of the chip assembly, and encapsulation of connections.

The quality of welded joints and, subsequently, the entire module depends on the stable repeatability of the ultrasonic welding process, which entails high requirements for the precision of manufacturing equipment used for ultrasonic welding of a microstrip sensor. The working plane of the equipment was mea-

sured before assembling the sensors in order to enter correction values into the welding program. The plane-parallelism of the equipment in the ultrasonic welding zone of the microstrip sensor is $\sigma = 10\text{--}20\ \mu\text{m}$, which is four times less than the minimum permissible value for the Delvotec G5 ultrasonic machine. In the design of the equipment, micrometric screws are used to adjust the sensor relative to the microcircuit with an accuracy of $3\text{--}5\ \mu\text{m}$. This allows one to collinearly set the position of the contact pads on the sensor relative to the pads on the chip with an accuracy of $3\text{--}5\ \mu\text{m}$, which greatly simplifies the assembly process with long microcables. The process and result of ultrasonic welding of a flexible microcable with a sensor is presented in Fig. 12.

After assembly, the quality of welded joints is tested using the same method as in the previous stage. The specifications of the sensor are considered during the assembly process of the module. There may be three main types of defects in the sensor (short circuit of the metallization layers of the microstrips, rupture of the microstrips, and breakdown of the MOS capacitor). If we use the specifications of the sensor during the assembly process, microstrips with broken capacitors do not become welded. If there is a group of short-circuited microstrips, only the central microstrip is assembled. Microstrips with defects in the metallization structure are assembled according to a standard technological process.

Figure 13 shows the results of testing one STS-XYTER chip with a microcable and a microstrip sensor. A comparison of the measurement results before and after assembly of the sensor (Figs. 13b, 13c)

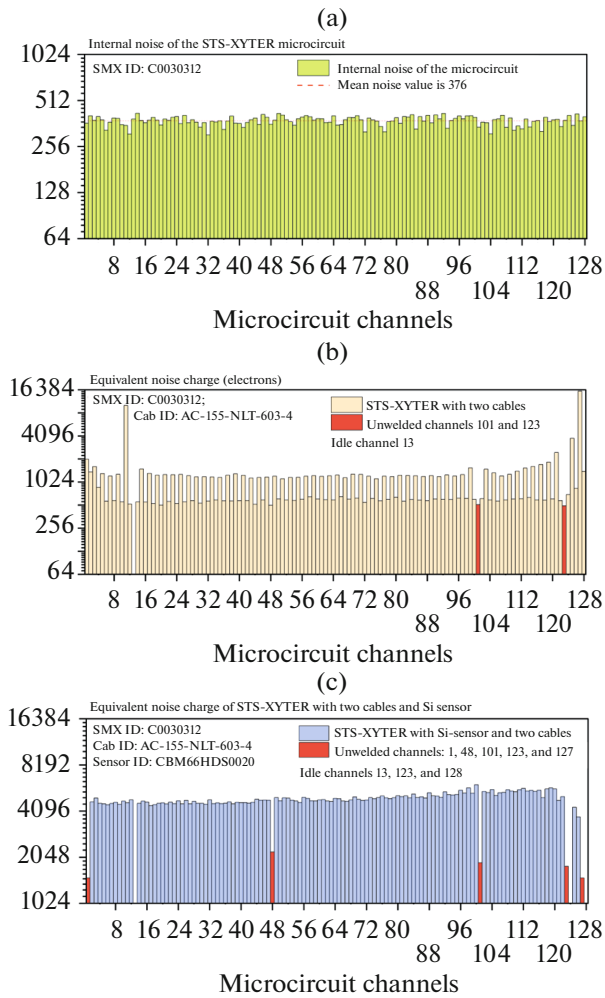


Fig. 13. Results of intermediate electrical testing of the STS-XYTER microcircuit during assembly with a microstrip sensor. (a) The intrinsic noise of the STS-XYTER microcircuit before ultrasonic welding of the cable to the input of the microcircuit and (b) the result of measuring noise in the channel of the readout electronics with assembled microcables. The noise difference between even microcable and odd microcable is due to the fact that the upper microcable acts as a shield for the lower cable. An increase in noise in channel 11 is due to capacitive coupling with idle channel 13. Figure 13c shows the result of measuring noise in the channels of a microcircuit with an assembled silicon sensor; measurements are in a test box without a shield on microcables and without bias voltage on the sensor, since the silicon sensor is not removed from the equipment during the assembly and there is no way to apply bias voltage. The results of testing the sensor with bias voltage are presented in Fig. 20.

showed that two idle channels (123 and 128) and three unwelded channels were added after assembly.

This microcircuit–microcable–sensor assembly and testing technique allows one to effectively identify idle channels at the ultrasonic welding stage, which makes the assembly repairable (the ability to repair ultrasonic joints before final encapsulation), thereby

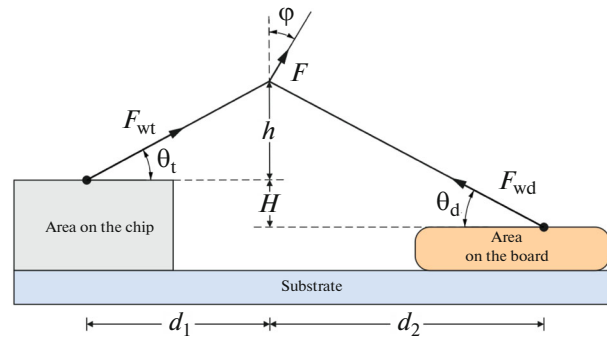


Fig. 14. Geometric variables for calculating ultrasonic joint parameters.

reducing the number of spare components used in the manufacturing of the tracking module.

Installation and Welding of ASIC on FEB Interface Boards: Selection of Ultrasonic Welding Parameters and Mechanical Testing after Assembly

Installing the STS-XYTER chip on the readout electronics board is the most important stage in the assembly process of the microstrip module. In this process, much attention is paid to ultrasonic welding of the microcircuit onto the board, because, if assembly will be unsuccessful, 128 channels are lost in the tracking module at once. Precisely selecting ultrasonic welding parameters and connecting loop geometry, as well as mechanical testing after assembly, guarantee high reliability and a long MTBF of the microstrip module.

The topology of the board in the area where the chip is installed was designed in such a way as to make the distances from the welding points between the pad on the chip and the board as equal as possible. Each STS-XYTER chip has 87 jumpers with a minimum distance of 950 μm and a maximum distance of 1150 μm . The loop parameters that were used in ultrasonic wedge–wedge welding are presented in Fig. 14.

The minimum tensile strength for 25 μm wire is ~ 8 cN [19]. The result of high-quality assembly of a microcircuit with a board is an indicator for measuring the tear force \vec{F} , which is the vector sum of forces \vec{F}_{wd} (tear force from the pad on the board) and \vec{F}_{wt} (tear force from the pad on the chip) (Fig. 14). The optimal selection of loop characteristics requires calculating the tear force of the welded joint from the pad on the chip \vec{F}_{wt} and on the board \vec{F}_{wd} . Finding the correct ratio of forces acting on welded joints at the welding points on the chip \vec{F}_{wd} and on the board \vec{F}_{wt} will help to get closer to the maximum values of the tear force. Maximum tear force will help achieve the best ultrasonic connection between the chip and the pad on the

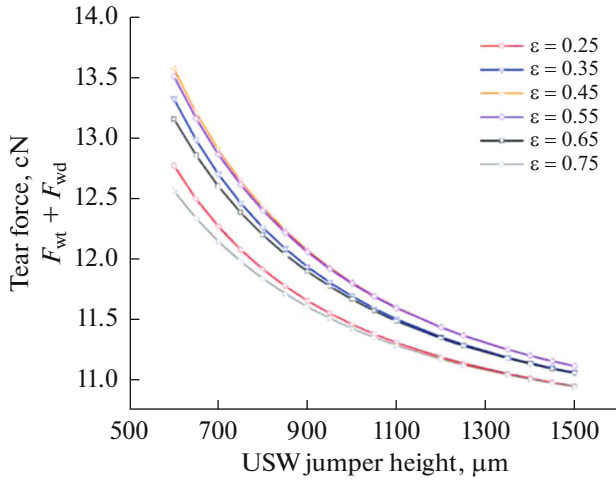


Fig. 15. Dependence of the tear force on the USW jumper height for different ratios between two connection points.

board, thereby guaranteeing the best mechanical properties of the tracking module after assembly.

The horizontal distance between the connection points (ε) on the chip and the pad is measured as the ratio of d_1 (the distance from the welding point on the chip to the point of application of the tear force) to d_2 (the distance from the welding point on the board to the point of application of the tear force). The distance between two connection points with different heights varies in the range of $1/4 \leq \varepsilon \leq 3/4$.

Since the welding points on the chip and the board are at different levels relative to the substrate, the tear forces will not be equal; $\overline{F_{wt}} \neq \overline{F_{wd}}$. The calculation of forces at the angle of tensile connection with respect to the substrate ($\varphi = 0^\circ$) (Fig. 14) is carried out according to the formulas [20]

$$F_{wt} = F \left[\frac{1 - \varepsilon}{\left(1 + \frac{\varepsilon H}{h}\right)} \left(1 + \frac{\varepsilon^2 d^2}{h^2}\right)^{1/2} \right], \quad (1)$$

$$F_{wd} = F \left[\frac{\varepsilon \left(1 + \frac{H}{h}\right)}{1 + \frac{\varepsilon H}{h}} \left(1 + \frac{(1 - \varepsilon)^2 d^2}{(h + H)^2}\right)^{1/2} \right], \quad (2)$$

where H is the height difference between two welding points on the board and the chip, h is height from the first welding point to the point of force application, d is total distance of the welded joint, and ε is ratio of horizontal distances between connection points.

The dependence of the tear force on the height of the jumper for a maximum welding length between the board and the microcircuit of 1150 μm for different values of ε with the tensile bond angle relative to the substrate ($\varphi = 0^\circ$) is shown in Fig. 15. The highest value of the tear force can be achieved at $\varepsilon = 0.45$.

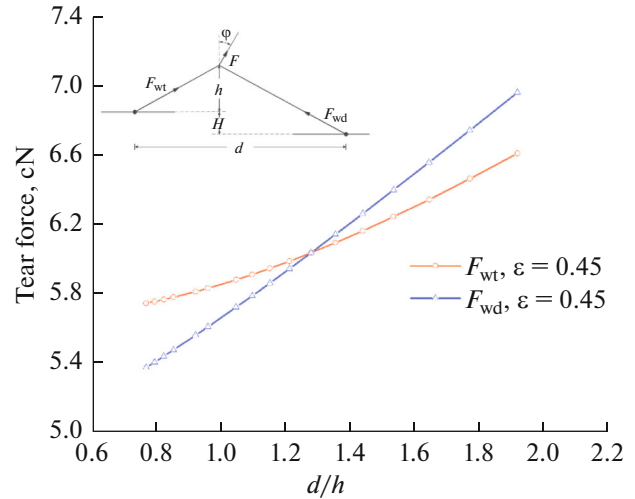


Fig. 16. Dependences of the tear force at points $\overline{F_{wt}}$ and $\overline{F_{wd}}$ on the geometric parameters of the welding loop at $\varepsilon = 0.45$ and the tensile bond angle relative to the substrate ($\varphi = 0^\circ$).

The best result of ultrasonic welding will be with equal values of the force to tear off the loop at the welding points on the board and the microcircuit. During the assembly process, the STS-XYTER chip is glued to the base of the board and the height difference between the two welding points on the board and the chip (H) for all jumpers is 200 μm . The separation parameters will be significantly influenced by the variables h , d_1 , and d_2 . The dependence of the tear force on the board $\overline{F_{wd}}$ and on the microcircuit $\overline{F_{wt}}$ on the geometric parameters of the welding loop with a ratio of horizontal distances between connection points of $\varepsilon = 0.45$ is shown in Fig. 16.

The same distribution of tear forces $\overline{F_{wt}} = \overline{F_{wd}} = 6.032$ cN is achieved with a value of $d/h = 1.27$. For a maximum welding loop length of 1150 μm , the distances are $d_1 = 402$ μm and $d_2 = 748$ μm (Fig. 14). The parameters are used to configure the Delvotec G5 ultrasonic automatic welding before assembling the STS-XYTER chip onto the FEB board.

The calculated value of the tear force obtained using formulas 1 and 2 is 12.06 g. Each STS-XYTER chip has additional contact test pads on which the ultrasonic welding mode is preselected. The mean tear force obtained from measuring the batch of assembled modules is 10.46 ± 0.22 g with a confidence interval of 95%. The results of measuring the tear force obtained during the assembly of the modules are presented in Fig. 17.

A high-quality joint of an ultrasonic wire with a diameter of 25 μm is considered to be a value greater than 8 g [19]. Based on the practical results, we can conclude that the mechanical connection between the

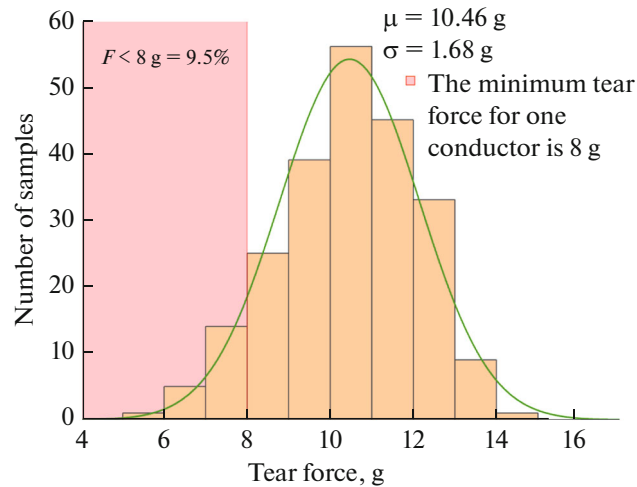


Fig. 17. Tear tests of aluminum wire (25 μm) welded using the wedge–wedge technology.

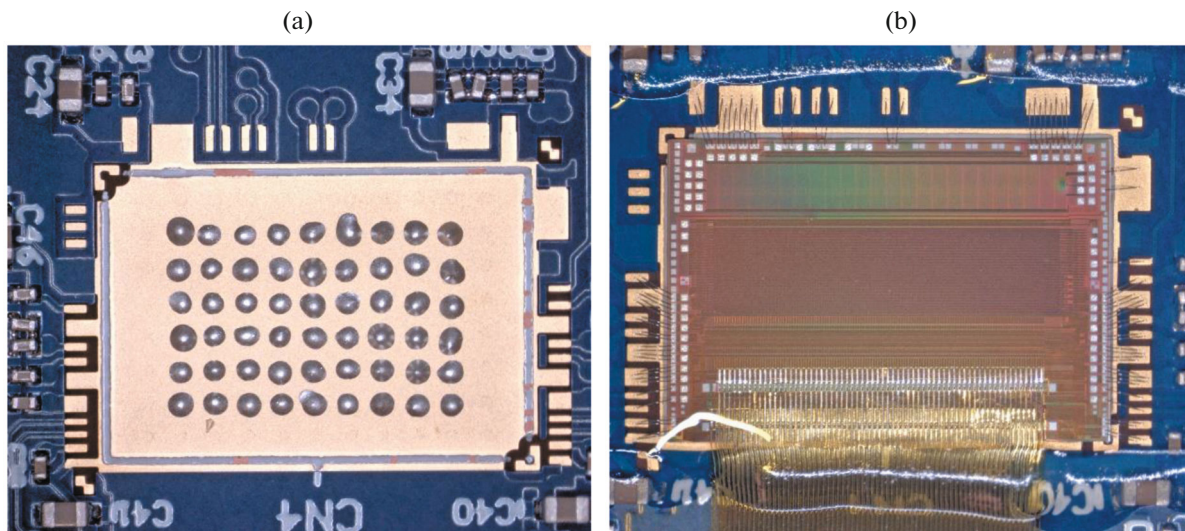


Fig. 18. Stages of installing the STS-XYTER ASIC reading electronics chip on the board. (a) Electrically conductive adhesive applied to the installation site of the microcircuit and (b) STS-XYTER chip with ultrasonic connection after encapsulation.

microcircuit and the board satisfies the requirements. The calculated value for tearing differs from that obtained during the assembly process by 15%, since when the conductor is torn off, the tool for tearing is positioned manually, which significantly affects the accuracy of finding the center of the ultrasonic jumper in real measurements.

The STS-XYTER microcircuit is installed in several stages. They are applying thermally conducting adhesive⁸ to the places for installing chips (Fig. 18a), polymerization of the adhesive in an oven at a temperature of 120°C, ultrasonic welding of the microcir-

cuit to the board, mechanical testing of ultrasonic joints for tearing, encapsulation with ultraviolet glue for mechanical protection and protection from external factors (moisture, dust, etc.) (Fig. 18b), and the installation of a protection shield.

Testing Tracking Modules after Assembly

Each tracking module is installed on a carrier frame (Fig. 19), which is equipment for storage and testing. The frame includes a water-cooled radiator, which provides the necessary heat removal from the module's readout electronics, the heat dissipation of which is ~ 24 W.

⁸ Epoxy Technology Epo-Tek[®] H20E Electrically Conductive, Silver Epoxy.

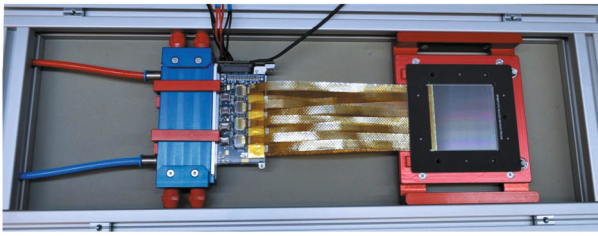


Fig. 19. Tracking module without installed shields on the testing equipment. The readout electronics boards are attached to a radiator for cooling during testing.

During testing, information (power consumption of each interface board with readout electronics, leakage current at a bias voltage of $V_{\text{bias}} = 100$ V, addresses of idle channels and channels with increased noise, and chip temperature) is entered into the CMIS [15]. The ADC and fast channel discriminator thresholds used to generate the hit timestamp are calibrated for each individual channel of all ASIC. Calibration files and files with channel masks are entered into CMIS and are used later when configuring the module as part of the tracking system. After functional testing and calibrating, a 24-h test is carried out with a Ru^{106} beta source, during which the response of each channel, the spread of channel gains, and the long-term operation performance of the module are measured.

One of the most important stages of testing is the stage of measuring the noise level in each individual channel with an offset sensor. An example of the noise distribution in the channels for one of the modules is shown in Fig. 20. A low noise level indicates a low input capacitance at the input of the CSA; that is, there is no an electrical connection at one of the two ends of the microcable. A zero noise on the graph indicates there are no noise hits in the channel, which is generally due to the nonfunctioning analog part of the microcircuit channel. The higher noise level in channels (1–128) on the p side corresponds to the noise of the microstrips on the sensor connected using a second metallization layer and therefore having a larger capacitance. The mean noise level is determined by the capacitance of the sensor strip and the capacitance of the microcable strip line [13] and should be no more than $1500 e^-$. The noise level can be affected by technological operations such as applying adhesive (encapsulation) and installing electromagnetic shields.

At the next stage, the module is tested with a radioactive source to check the welding map and determine the spread of gain factors in the sensor channels. An example of measurement results is shown in Fig. 21. The spread of gain factors in channels on one side of the sensor is no more than 15%.

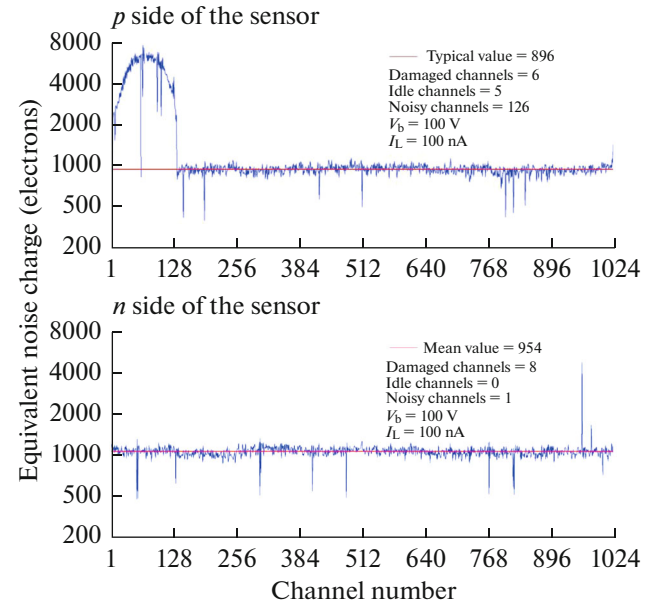


Fig. 20. Measurements of noise in the channels of the tracking module on p side and n side. The increased noise level in channels (1–128) on the p side of the sensor is due to z microstrips (see Fig. 2) and double metallization on the sensor.

Preliminary Production Assembly of Modules

The total number of assembled modules is 25 pieces. To debug assembly procedures and evaluate the yield of suitable modules, a preproduction assembly of the first batch of eight tracking modules was carried out using a new type of equipment and ultrasonic welding modes.

The following requirements apply to modules that qualify as suitable for manufacturing a tracking system (Fig. 22).

- (1) The number of idle channels on each side of the sensor is no more than 1.5%.
- (2) The total number of idle channels is no more than 3%.
- (3) The number of adjacent idle channels in a group is no more than 5 pieces.
- (4) The module must successfully pass all stages of QA testing.

A group of four people is involved in the assembly process; the working time of one shift is 7 h. In one process, four modules are assembled in parallel. The mean time required to assemble one module is 22.5 h. The yield of suitable modules in the preproduction batch is 87.5%.

The assembly time of tracking modules can be reduced by 15% by increasing the number of ultrasonic welding machines while separating TAB and wire welding.

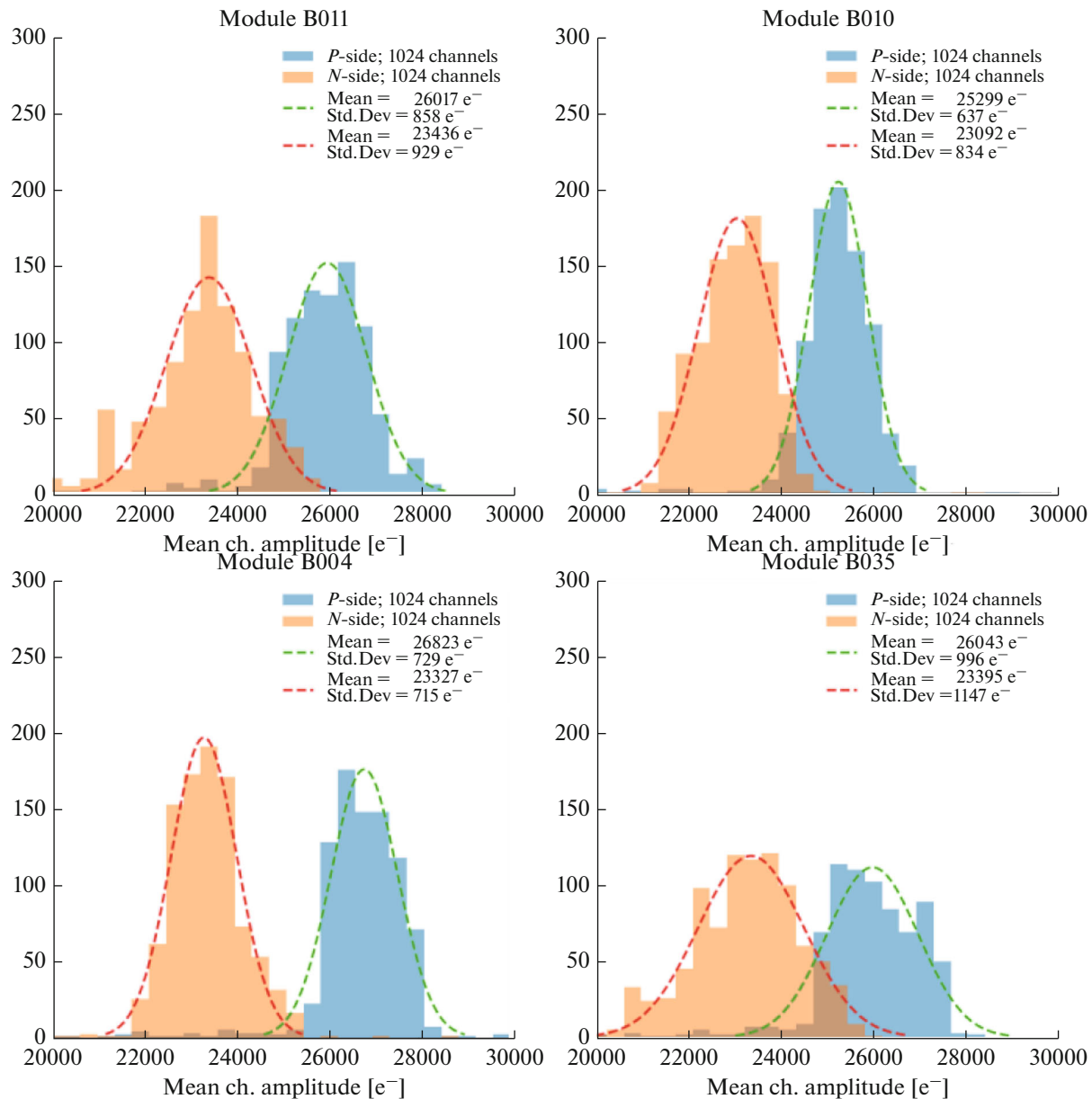


Fig. 21. Dispersion of gain factors from 1 MIP in sensor channels for different modules (single-strip cluster).

The results of assembly of tracking modules with the number of idle channels in the module are presented in Fig. 23.

CONCLUSIONS

We have developed a methodology for assembling tracking modules with double-sided silicon strip sensors with ultralight polyimide-based aluminum microcables using test benches for intermediate mechanical and functional testing. The method for determining the optimal parameters for ultrasonic welding with aluminum wire is described in detail. The results of using ultrasonic TAB technology in the

assembly of tracking modules are presented. This method of selecting parameters made it possible to obtain a mean value (4.6 g) of the tear force for an aluminum conductor with a thickness of 14 μm and a width of 40 μm .

The calculation of geometric parameters for welding technology with aluminum wire allowed us to achieve a mean value of the tear force of 10.46 ± 0.22 g for welding with 25 μm wire.

Laboratory tests of the tracking module showed that the mean equivalent noise charge for the p side is $896 e^-$, and the mean equivalent noise charge for the n side is $954 e^-$. Testing of the modules using a 1 GeV proton beam showed that the mean electron level for

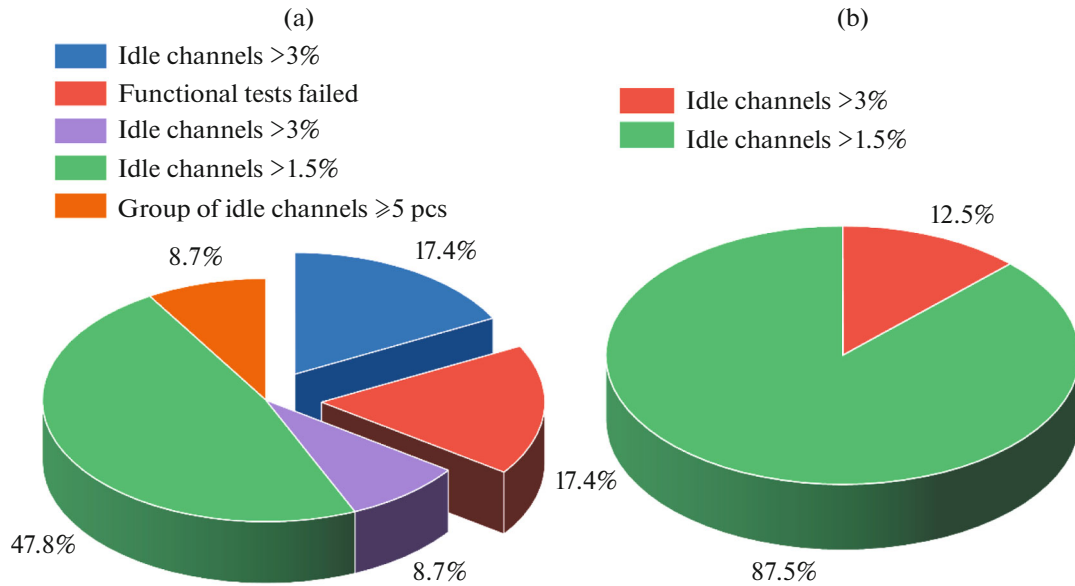


Fig. 22. Results of assembly of tracking modules. (a) Total number of assembled modules (23) and (b) results of assembly of a preproduction batch of tracking modules (8).

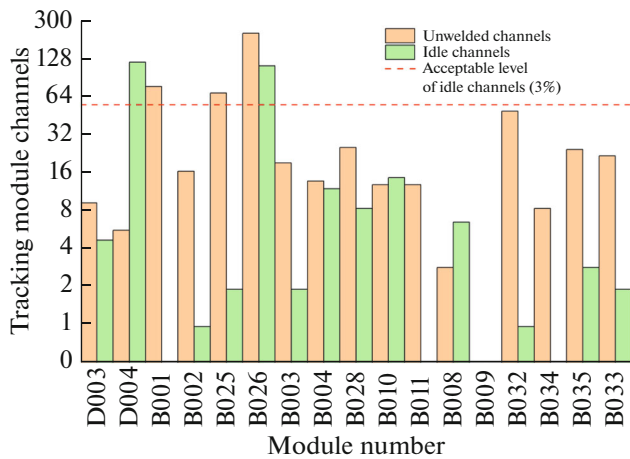


Fig. 23. Number of idle channels and unwelded channels in tracking modules of preproduction assembly (8 pcs.). The yield of suitable tracking modules is 88.3%.

the minimum ionizing particle is $\sim 26000 e^-$ for the p side of the sensor and $\sim 23000 e^-$ for the n side of the sensor.

A preliminary assessment of the assembly area’s performance was based on the preproduction assembly of a batch of eight modules. The yield of suitable modules is 88.3%. The mean time to assemble one module is 22.5 h. Thus, the assembly of 292 modules at one assembly site using one shift will take 3.5 years. To increase the productivity of the module assembly site many times over, it is necessary to introduce additional shifts and train the necessary workers.

FUNDING

This work was supported by ongoing institutional funding. No additional grants to carry out or direct this particular research were obtained.

CONFLICT OF INTEREST

The authors of this work declare that they have no conflicts of interest.

REFERENCES

1. R. Angstadt et al., “The layer 0 inner silicon detector of the D0 experiment,” *Nucl. Instrum. Meth. Phys. Res., Sect. A* **622**, 298–310 (2010).
2. S. Abachi et al., “The D0 Detector,” *Nucl. Instrum. Meth. Phys. Res., Sect. A* **338**, 185–253 (1994).
3. P. Kuijser, “The ALICE silicon strip detector system,” *Nucl. Instrum. Meth. Phys. Res., Sect. A* **447**, 251–256 (2000).
4. *Handbook of Tape Automated Bonding*, Ed. J. H. Lau (Van Nostrand Reinhold, New York, 1982).
5. B. Friman et al., *Compressed Baryonic Matter in Laboratory Experiments* (P. Senger, Berlin, 2011), Vol. 814.
6. A. Baranov et al., *The Silicon Tracking System as a Part of Hybrid Tracker of BM@N Experiment* (Dubna, 2020).
7. J. Heuser et al., “Technical design report for the CBM silicon tracking system (STS),” (GSI, Darmstadt, 2013).
8. O. Bertini, “Production readiness review for the silicon sensors of the CBM silicon tracking system,” Technical Note CBM-TN-18010 (Germany, 2013).
9. V. Borshchov et al., “Development of thin multi-line cables for the STS micro-strip detector modules,” CBM Progress Report 2007 (Germany, 2008).

10. I. Panasenkov et al., “Microcable quality assurance: capacitance measurements” (Darmstadt, Germany, 2017).
11. M. Shitenkov et al., “Front-end electronics for BM@N STS,” *Phys. Part. Nucl.* **52**, 826–829 (2021).
12. K. Kasinski et al., “Characterization of the STS/MUCH-XYTER2, a 128-channel time and amplitude measurement IC for gas and silicon microstrip sensors,” *Nucl. Instrum. Meth. Phys. Res., Sect. A* **908**, 225–235 (2018).
13. D. V. Dement’ev et al. “Signal/noise ratio of the silicon tracking system module of the BM@N experiment,” *Prib. Tekh. Eksp.*, No. 1, 23–32 (2023).
14. A. Sheremetev, R. Arteché Diaz, and M. Shitenkov, “QA tests of the LDOs developed for the assembly of the BM@N STS modules” (Darmstadt, 2022).
15. C. Ceballos et al., “Construction management information system at JINR,” *Phys. Part. Nucl. Lett.* **20**, 981–987 (2023).
16. M. Lindgren, I. Belov, and P. Leisner, “Experimental evaluation of glob-top materials for use in harsh environments,” *J. Microelectron. Electron. Packag.* **2**, 253–268 (2005).
17. Department of Defense US. MIL-STD-883 Test Method Standard for Microcircuits (1996).
18. A. Sheremetev et al., “The quality assurance test system for assembly of STS modules for the BM@N experiment,” *Phys. Elem. Part. At. Nucl.* **20**, 613–618 (2023).
19. Testing of wire bonds (CERN). https://bondlab-qa.web.cern.ch/Pull_test.html.
20. W. M. Bullis, *Semiconductor Measurement Technology: The Destructive Bond Pull Test* (U.S. Gov. Print. Office, Washington, DC, 1976).

Translated by I. Obrezanova

Publisher’s Note. Pleiades Publishing remains neutral with regard to jurisdictional claims in published maps and institutional affiliations.